

PROCEEDINGS OF SPIE

[SPIDigitalLibrary.org/conference-proceedings-of-spie](https://spiedigitallibrary.org/conference-proceedings-of-spie)

Classification of the polarization properties of polycrystalline networks of biological fluid films

Mishalov, Volodymyr, Bachinsky, Viktor, Vanchulyak, Oleg Ya., Zabolovitch, Alina, Sarkisova, Yuliya, et al.

Volodymyr D. Mishalov, Viktor T. Bachinsky, Oleg Ya. Vanchulyak, Alina Y. Zabolovitch, Yuliya V. Sarkisova, Alexander G. Ushenko, Olexander V. Dubolazov, Nataliia I. Zabolotna, Vladimir A. Ushenko, Yaroslav M. Drin, Valentina Dvorjak, Andrzej Kotyra, Mashat Kalimoldayev, "Classification of the polarization properties of polycrystalline networks of biological fluid films," Proc. SPIE 11581, Photonics Applications in Astronomy, Communications, Industry, and High Energy Physics Experiments 2020, 115811I (14 October 2020); doi: 10.1117/12.2580706

SPIE.

Event: Photonics Applications in Astronomy, Communications, Industry, and High Energy Physics Experiments 2020, 2020, Wilga, Poland

Classification of the polarization properties of polycrystalline networks of biological fluid films

Volodymyr D. Mishalov*^a, Viktor.T. Bachinsky^b, Oleg Ya. Vanchulyak^b, Alina Y. Zavolovitch^b, Yuliya V. Sarkisova^b, Alexander G. Ushenko^c, Olexander V. Dubolazov^c, Natalia I. Zabolotna^d, Vladimir A. Ushenko^c, Yaroslav M. Drin^c, Valentina Dvorjak^c, Andrzej Kotyra^e, Mashat Kalimoldayev^f

^aShupyk National Medical Academy of Postgraduate Education, 9, Dorogozhytska St., Kyiv, 04112, Ukraine; ^bBukovinian State Medical University, Teatral'na Square, 2, 58000 Chernivtsi, Ukraina; ^cChernivtsi National University, Kotsyubynsky 2, 58012 Chernivtsi, Ukraine; ^dVinnitsia National Technical University, Khmel'nyts'ke Hwy, 95, 21000 Vinnitsia, Ukraina, ^eLublin University of Technology, Nadbystrzycka 38D, 20-618 Lublin, Poland; ^fInstitute of Information and Computational Technologies CS MES RK, 050010 Almaty, 125 Pushkina, Republic of Kazakhstan

ABSTRACT

The results of a complex statistical, correlation and fractal analysis of distributions of the magnitude of the real component of the elements of the Jones matrix polycrystalline films of biological fluids of different biochemical composition are presented. The magnitudes and ranges of changes in the set of statistical, correlation, and fractal moments of the 1st to 4th orders, which characterize the Jones-matrix images of dendritic, spherulithic, and combined networks of biological crystals, are determined. A classification system is proposed for the polarization manifestations of the optically anisotropic properties of such polycrystalline structures for the development of the principles for the differential diagnosis of pathological conditions of human organs.

Keywords: polarization, interference, anisotropy, cartography

1. INTRODUCTION

Our work is devoted to the development and experimental testing of the laser mapping method of polycrystalline films of biological fluids using the formalism of Jones matrices¹⁻³. As objects of study, we used smears of biological fluids of a healthy human body^{4,5}:

- saliva (21 samples) - group 1;
- blood plasma (21 samples) - group 2;
- bile (21 samples) - group 3;
- synovial fluid (21 samples) - group 4.

This choice of body fluids is due to the following factors⁶⁻¹⁰:

- they cover a wide range of physiological functions of the human body;
- diverse biochemical structure has common optical manifestations of anisotropy (saliva - liquid crystals of albumin and globulin; blood plasma - liquid crystals of fibrin, as well as amino acids of albumin and globulin, and fibrin; bile - liquid and solid calcium bilirubinate and fatty acids; synovial fluid - collagen and fibrin liquid crystals);
- other physiologically important types of biological fluids (transudate and exudates, effusion, liquor, lymph, pulmonary condensate, etc.) are, to a certain extent, a combination of the optical-anisotropic properties of samples of mentioned groups^{6,7,11}.

2. JONES-MATRIX IMAGES OF SALIVA

In order to obtain objective criteria for the classification of manifestations of the optical anisotropy of polycrystalline networks of biological fluid films of group 1 (21 samples), we conducted a comprehensive study of the coordinate

* inter-dep@nmapo.edu.ua

distributions of the real component of the elements of the Jones matrix $R_{11}(m \times n)$ and $R_{12,21}(m \times n)$, which mainly characterize the manifestations of the orientational $R_{12,21}(m \times n)$ and phase δ structure of the biological crystal ensemble⁶⁻⁸.

Within group 1, the statistically averaged values and the variance of the variation of the set of parameters characterizing the real component of the Jones-matrix images were determined $R_{11}(m \times n)$ and $R_{12,21}(m \times n)$:

- statistical moments of the 1st - 4th orders M ; σ ; A ; E ;
- correlation moments of the 1st - 4th orders $K_{i=1;2;3;4}$;
- spectral moments of the 1st - 4th orders $K_{i=1;2;3;4}$.

In fig. 1 and fig. 2 shows a series of coordinate distributions of elements of the Jones matrix $R_{11}(m \times n)$ (Fig. 1) and $R_{12,21}(m \times n)$ (Fig. 2) and the corresponding histograms $N(R_{11})$, $N(R_{12,21})$, the autocorrelation functions $G_{11}(\Delta x)$, $G_{12,21}(\Delta x)$, and the logarithmic spectral dependences $LgJ(G_{11})$, $LgJ(G_{12,21})$ of such distributions.

The results of the study of Jones-matrix images of the actual component of the elements of the polycrystalline network of biological crystals of an optically thin layer of saliva indicate a sufficient level of optical anisotropy. This fact is indicated by the wide range ($0 \leq \Delta R_{11} \leq 1$) of the eigenvalues of the matrix element $R_{11}(m \times n)$. Moreover, the histogram $N(R_{11})$ is characterized by the predominance (2–7 times) of the probabilities of the values of the “orientational” matrix element compared with the values of other extremes (Fig. 1).

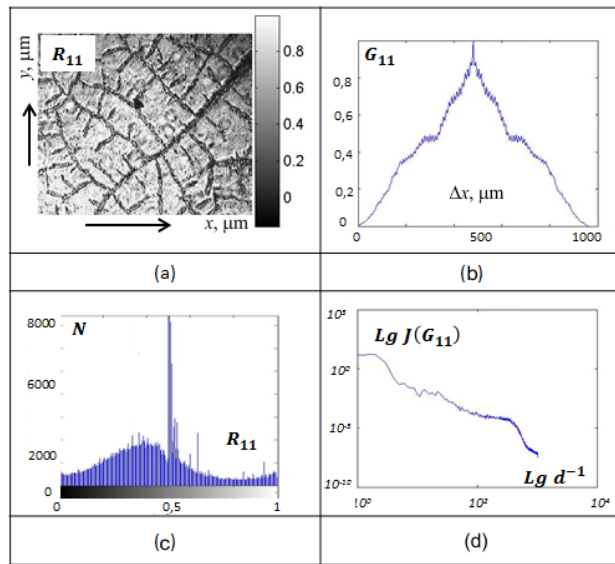


Figure 1. Coordinate (a), correlation (b), probabilistic (c) and self-similar (d) structure of the real component of the element of the Jones matrix R_{11} of a polycrystalline network of a human saliva layer

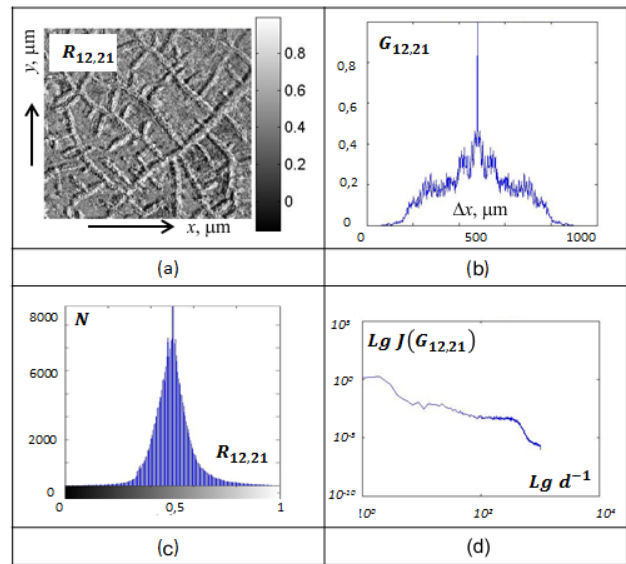


Figure 2. Coordinate (a), correlation (b), probabilistic (c) and self-similar (d) structure of the real component of the element of the Jones matrix $R_{12,21}$ of a polycrystalline network of a human saliva layer

The histogram $N(R_{12,21})$ of the distribution of values of the real component of this element is symmetric with respect to the main extremum (Fig. 2), which confirms the assumption that the morphological structure of the optically anisotropic polycrystalline network of the saliva layer contains protein structures of the same biochemical composition¹¹.

The correlation approach to the analysis of the obtained results revealed that the autocorrelation functions $G_{1;12;21}(\Delta x)$ are falling dependencies with pronounced fluctuations of eigenvalues (Fig. 1 and Fig. 2).

The sets of values of the real component of the elements of the Jones matrix are multifractal. The corresponding logarithmic dependences $\lg J(G_{11})$; $\lg J(G_{12,21})$ are characterized by broken approximate curves with three angles of inclination. This fact can be associated with multiple discrete changes in the orientation of the optical axes of partial biological crystals with a simultaneous multiple change of the phase period δ . Therefore, the coordinate distributions of the real component of the elements $R_{ik}(x, y)$ of the generalized Jones matrix operator are quasi-harmonic dependences with several basic fluctuation frequencies, which is the reason for the formation of a set of self-similar sets $R_{ik}(x, y)$ on different geometrical scales of polycrystalline network group 1. The results of the quantitative analysis of the values and ranges of change of the statistical, correlation and spectral moments²⁻⁷ coordinate distributions $R_{ik}(x, y)$ are given in Table 1.

Tabela 1. Statistical (M , σ , A , E), correlation ($K_{i=1;2;3;4}$), spectral ($S_{i=1;2;3;4}$) parameters of Jones-matrix images $R_{ik}(m \times n)$ of polycrystalline networks of saliva of healthy people (21 samples)

Options	$R_{11}(m \times n)$	$R_{12,21}(m \times n)$
M	$0,54 \pm 0,12$	$0,15 \pm 0,036$
σ	$0,43 \pm 0,092$	$0,17 \pm 0,039$
A	$1,26 \pm 0,41$	$0,43 \pm 0,055$
E	$3,17 \pm 0,075$	$0,61 \pm 0,21$
K_1	$0,41 \pm 0,086$	$0,49 \pm 0,11$
K_2	$0,25 \pm 0,062$	$0,12 \pm 0,028$
K_3	$5,28 \pm 1,11$	$0,68 \pm 0,13$
K_4	$1,86 \pm 0,32$	$2,41 \pm 0,72$
S_1	$0,51 \pm 0,13$	$0,63 \pm 0,19$
S_2	$0,27 \pm 0,061$	$0,17 \pm 0,044$
S_3	$0,39 \pm 0,085$	$0,23 \pm 0,061$
S_4	$0,57 \pm 0,14$	$0,43 \pm 0,093$

As can be seen, the values of all statistical moments M , σ , A , E , characterizing the coordinate distributions of the elements of the Jones matrix $R_{ik}(m \times n)$, which are different from zero. Moreover, extremely large values are inherent in the statistical moment of the 4th order. In other words, the probability distributions of the values of the real component of the Jones matrix of the dendritic polycrystalline network of an optically thin layer of saliva are quite complex and differ significantly from those known in the theory of mathematical statistics — normal or Gaussian. The correlation moments of the 3rd and 4th orders of the autocorrelation dependences $G_{1,1;2,21}(\Delta x)$ of the distribution of values $R_{1,1;2,21}(m \times n)$ turned out to be no less informative - their value is one order of magnitude larger than the correlation moments of the 1st and 2nd orders.

A comparative analysis of the set of spectral moments $S_{i=1;2;3;4}$ of the logarithmic dependences of the power spectra of the distributions of the real component of the elements of the Jones matrix also revealed a difference from zero and a significant range of changes in their values.

3. JONES-MATRIX IMAGES OF BLOOD PLASMA

In fig. 3 and fig. 4 shows a series of coordinate distributions of the real component of the Jones matrix elements $R_{11}(m \times n)$ (Fig. 3) and $R_{12,21}(m \times n)$ (Fig. 4) the spherulithic albumin-globulin network of blood plasma and the

corresponding histograms $N(R_{11})$, $N(R_{12,21})$, autocorrelation functions $G_{11}(\Delta x)$; $G_{12,21}(\Delta x)$, logarithmic spectral dependences $LgJ(G_{11})$; $LgJ(G_{12,21})$ of such distributions.

The results of the study of the polarization properties of the polycrystalline network of albumin and globulin of an optically thin layer of blood plasma indicate a significant influence of the structure of the coordinate distributions of the real component of the elements, both the features of the distribution of the directions of the optical axes of biological crystals and the birefringence of their substance. This fact is indicated by the widest range of variation ($0 \leq \Delta R_{11} \leq 1$) of the eigenvalues of the distribution $R_{11}(m \times n)$ with fairly close probabilities of different values of the corresponding matrix element (Fig. 3).

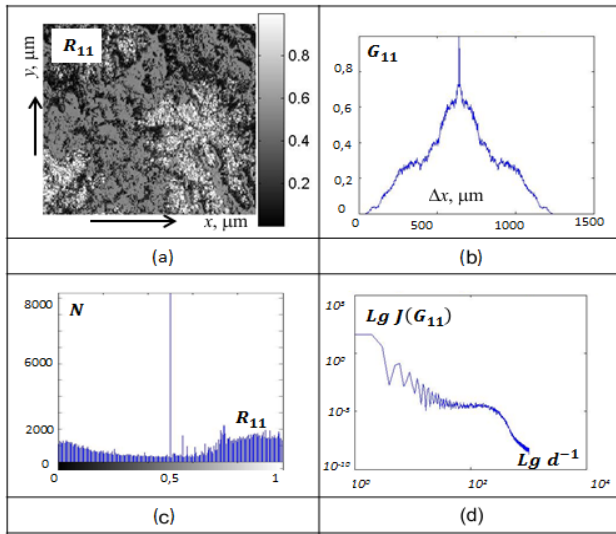


Figure 3. Coordinate (a), correlation (b), probabilistic (c) and self-similar (d) structure of the actual component of the element of the Jones matrix R_{11} of the polycrystalline network of human blood plasma

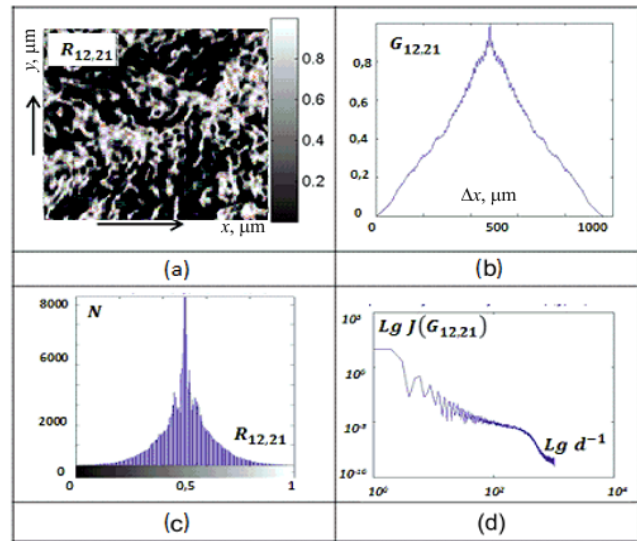


Figure 4. Coordinate (a), correlation (b), probabilistic (c) and self-similar (d) structure of the actual component of the element of the Jones matrix $R_{12,21}$ of the polycrystalline network of human blood plasma

Another dependence occurs for the histogram of the distribution of values of the real component $R_{12,21}$. As can be seen from fig. 4 $N(R_{12,21})$, fairly symmetrical with respect to the main extremum. A comparative analysis with data on the phase-shifting ability of the dendritic polycrystalline network of the saliva layer (Fig. 2) revealed a large dispersion, indicating a larger range of variation in the geometric dimensions of the partial birefringent crystals that form one or another phase shift value δ .

The autocorrelation functions $G_{11,12,21}(\Delta x)$ of the real component of the Jones-matrix images $R_{ik}(m \times n)$ of plasma samples from group 2 are dropping dependencies with pronounced fluctuations of eigenvalues (Fig. 3 and Fig. 4). In addition, a discrete, scale-repeated change in the orientations of the optical axes of partial biological crystals with a simultaneous multiple change in the phase period is manifested in the formation of self-similar sets on different geometric scales of the polycrystalline network. As can be seen, the distribution of the values of the real component of the elements of the Jones matrix is multifractal. The corresponding logarithmic dependences $lgJ(G_{11})$; $lgJ(G_{12,21})$ are characterized by broken approximating curves with three angles of inclination.

The results of the quantitative analysis of the values and ranges of change of the statistical, correlation, and spectral moments of the coordinate distributions $R_{ik}(m \times n)$ are shown in table 2.

From the analysis of the obtained set of quantitative parameters characterizing the coordinate distributions of the real component of the elements of the Jones matrix, the spherulith network of biological crystals follows:

- sensitivity to changes in the geometric construction of a polycrystalline network of optical-uniaxial birefringent crystals of statistical, correlation and spectral moments of higher orders;

- differences in the statistical moments of the 3rd (2–3 times) and 4th (2–7 times) orders characterizing the distributions of the real component of the Jones matrix of the spherulite network compared with similar data for dendritic networks (table 1);
- the differences for the correlation moments are 2–5 times (K_3) and 2–4 times (K_4), respectively;

for the spectral moments of the 3rd and 4th orders of the logarithmic dependences of the power spectra of the real component of the matrix elements, the differences were revealed by 1.5 to 2 times.

Table 2. Statistical (M , σ , A , E), correlation ($K_{i=1;2;3;4}$), spectral ($S_{i=1;2;3;4}$) parameters of Jones-matrix images $S_{i=1;2;3;4}$ of polycrystalline plasma film networks, blood of healthy people (21 samples)

Options	$R_{11}(m \times n)$	$R_{12;21}(m \times n)$
M	$0,49 \pm 0,14$	$0,18 \pm 0,042$
σ	$0,38 \pm 0,089$	$0,24 \pm 0,053$
A	$2,77 \pm 0,72$	$0,76 \pm 0,38$
E	$1,89 \pm 0,48$	$0,72 \pm 0,68$
K_1	$0,44 \pm 0,098$	$0,48 \pm 0,099$
K_2	$0,12 \pm 0,029$	$0,18 \pm 0,042$
K_3	$2,46 \pm 0,68$	$0,48 \pm 0,075$
K_4	$3,08 \pm 0,57$	$2,39 \pm 0,55$
S_1	$0,54 \pm 0,072$	$0,69 \pm 0,088$
S_2	$0,14 \pm 0,031$	$0,21 \pm 0,041$
S_3	$0,34 \pm 0,067$	$0,31 \pm 0,078$
S_4	$0,41 \pm 0,91$	$0,52 \pm 0,11$

4. JONES-MATRIX IMAGES OF BILE

In fig. 5 and fig. 6 shows the coordinate distributions of the real component of the Jones matrix elements $R_{11}(m \times n)$ (Fig. 5) and $R_{12;21}(m \times n)$ (Fig. 6) of the optic-anisotropic structure of bile and the corresponding histograms $N(R_{11})$, $N(R_{12;21})$, autocorrelation functions $G_{11}(\Delta x)$; $G_{12;21}(\Delta x)$, logarithmic spectral dependences $LgJ(G_{11})$; $LgJ(G_{12;21})$ of such distributions.

The cluster structure of the crystalline component of the optically thin layer of bile is in the widest possible range of a fairly equally probable range of variation ($0 \leq \Delta R_{11} \leq 1$) of the eigenvalues of the distribution of the real component of the matrix element $R_{11}(m \times n)$ (Fig. 6). The histogram $N(R_{12;21})$ of the distribution of values of the real component $R_{12;21}$ of the Jones matrix element of the bile layer remains, as in the previous cases of dendritic (Fig. 2) and spherulite (Fig. 4) polycrystalline networks of biological crystals, quite symmetrical with respect to the main extremum. The autocorrelation functions $G_{11;12;21}(\Delta x)$ of the real component of the Jones-matrix images $R_{ik}(m \times n)$ of bile samples from group 3 are monotonically decreasing dependencies without fluctuations of eigenvalues (Fig. 5 and Fig. 6). In addition, a large-scale repetitive change in the orientation of the optical axes of partial biological crystals with a simultaneous multiple change of the phase period δ is manifested in the formation of self-similar sets on different geometric scales of the cluster polycrystalline network. The corresponding logarithmic dependences $lgJ(G_{11})$; $lgJ(G_{12;21})$ are characterized by broken approximate curves with three angles of inclination.

The results of the quantitative analysis of the values and ranges of change of the statistical, correlation, and spectral moments of the coordinate distributions $R_{ik}(m \times n)$ are shown in Table 3.

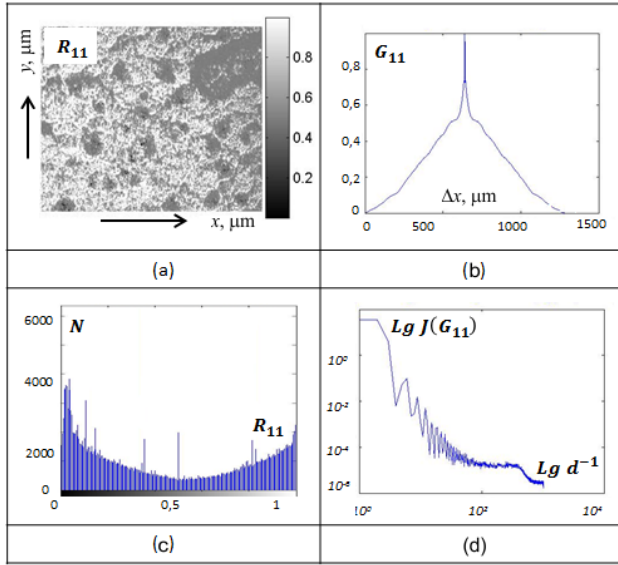


Figure 5. Coordinate (a), correlation (b), probabilistic (c) and self-similar (d) structure of the actual component of the element of the Jones matrix R_{11} of a human bile polycrystalline network

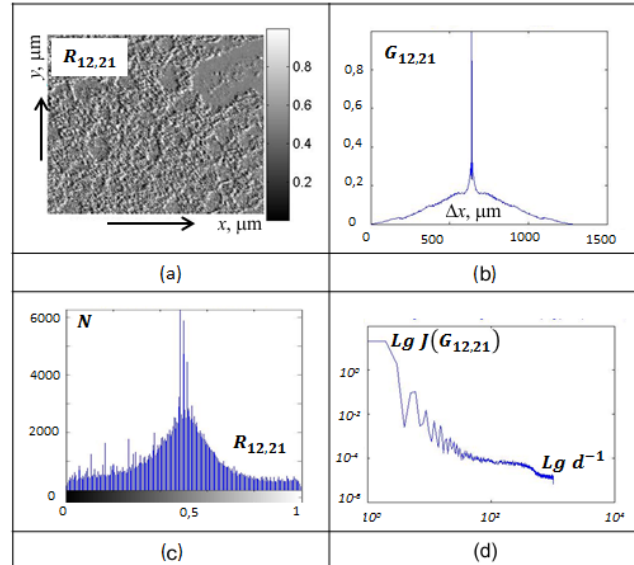


Figure 6. Coordinate (a), correlation (b), probabilistic (c) and self-similar (d) structure of the actual component of the element of the Jones matrix $R_{12,21}$ of a human bile polycrystalline network

Tabela 3. Statistical (M , σ , A , E), correlation ($K_{i=1;2;3;4}$), spectral ($S_{i=1;2;3;4}$) parameters of Jones-matrix images \aleph_{ik} ($m \times n$) of bile polycrystalline networks of healthy people (21 samples)

Options	$\aleph_{11} (m \times n)$	$\aleph_{12,21} (m \times n)$
M	$0,61 \pm 0,19$	$0,23 \pm 0,055$
σ	$0,49 \pm 0,12$	$0,31 \pm 0,069$
A	$0,45 \pm 0,097$	$0,97 \pm 0,19$
E	$0,89 \pm 0,13$	$0,85 \pm 0,33$
K_1	$0,51 \pm 0,105$	$0,57 \pm 0,15$
K_2	$0,29 \pm 0,072$	$0,21 \pm 0,47$
K_3	$1,19 \pm 0,34$	$0,56 \pm 0,13$
K_4	$5,88 \pm 1,44$	$2,12 \pm 0,49$
S_1	$0,58 \pm 0,16$	$0,72 \pm 0,16$
S_2	$0,29 \pm 0,71$	$0,21 \pm 0,077$
S_3	$0,48 \pm 0,11$	$0,29 \pm 0,085$
S_4	$0,79 \pm 0,18$	$0,47 \pm 0,091$

From the analysis of the obtained set of statistical, correlation and spectral parameters characterizing the coordinate distributions of the values of the real component of the Jones matrix elements formed by the "orientational" and "phase" effects of optical-anisotropic clusters of an optically thin layer of bile, the individual sensitivity to changes in the geometric construction of a polycrystalline network of higher moments orders. A further change in the statistical moments of the 3rd (2–3 times) and 4th (2–7 times) orders characterizing the distributions of the real component of the Jones matrix of the cluster network compared with similar data for dendritic and spherulithic networks (Table 1, table 2). The correlation moments differ 2.3 - 2.7 times (K_3) and 2.1 - 2.5 times (K_4), respectively. For the spectral moments of the 3rd (S_3) and 4th (S_4) orders of the logarithmic dependences of the power spectra of the real component of the matrix elements of various types $R_{ik}(\rho)$, $R_{ik}(\delta)$ differences were found in from 1.45 to 1.68 times.

5. CONCLUSIONS

For the first time for the classification of polarization manifestations of the optical anisotropy of polycrystalline networks of human biological fluids films, a comprehensive statistical, correlational and fractal scale-selective analysis of the coordinate structure of the real and imaginary component of Jones-matrix images was proposed. On this basis, the interrelations between the statistical, correlation, and spectral moments of the 1st - 4th orders were established, which characterize the coordinate distribution of the elements of the Jones matrix of the main types of films (saliva, blood plasma, bile) of human fluids, and symmetry (dendritic, spherulitic, cluster) birefringent polycrystalline networks of biological crystals.

The influence of the distributions of the directions of the optical axes and the birefringence of the multilayer polycrystalline network on the coordinate structure of the real component of the "orientational" and "phase" elements of the Jones matrix of films of the main types of biological fluids of man is analytically substantiated and experimentally detected. Based on this, the optical-physical criteria for the transformation of the type of spatial symmetry of the structure (dendritic - spherulitic - cluster) of polycrystalline networks of biological crystals were determined for the first time, and a system for classifying their optical properties was developed by estimating the ranges of variation of the statistical, correlation, and spectral moments of the 1st - 4th orders that characterize the real component of the Jones-matrix images of optically thin layers of body fluids.

REFERENCES

- [1] Ushenko, V. A., Koval, G. D., Gavrylyak, M. S., Mueller, "Matrices polarization selection of two-dimensional linear and circular birefringence images," *Proceedings of SPIE - The International Society for Optical Engineering* 8856, 88562E (2013).
- [2] Ushenko, V. O., "Spatial-frequency polarization phasometry of biological polycrystalline networks," *Optical Memory and Neural Networks (Information Optics)* 22(1), 56-64 (2013).
- [3] Kozlovska, T. I., Kolisnik, P. F., Zlepko, S. M., et al., "Physical-mathematical model of optical radiation interaction with biological tissues," *Proc. SPIE* 10445, (2017).
- [4] Prysyazhnyuk, V. P., Ushenko, Yu. A., Dubolazov, A. V., Ushenko, A. G., Ushenko, V. A., "Polarization-dependent laser autofluorescence of the polycrystalline networks of blood plasma films in the task of liver pathology differentiation," *Applied Optics* 55(12), B126-B132 (2016).
- [5] Ushenko, V. A., "Complex degree of mutual coherence of biological liquids," *Proceedings of SPIE - The International Society for Optical Engineering* 8882, 88820V (2013).
- [6] Ushenko, Y. A., Koval, G. D., Ushenko, A. G., Dubolazov, O. V., Ushenko, V. A., Novakovskaia, O. Y., "Mueller-matrix of laser-induced autofluorescence of polycrystalline films of dried peritoneal fluid in diagnostics of endometriosis," *Journal of Biomedical Optics* 21(7), 071116 (2016).
- [7] Angelsky, P. O., Ushenko, A. G., Dubolazov, A. V., Sidor, M. I., Bodnar, G. B., Koval, G., Trifonyuk, L., "The singular approach for processing polarization-inhomogeneous laser images of blood plasma layers," *Journal of Optics (United Kingdom)* 15(4), 044030 (2013).
- [8] Ushenko, O. G., Dubolazov, A. V., Balanets'ka, V. O., Karachevtsev, A. V., Sydor, M., "Wavelet analysis for polarization inhomogeneous laser images of blood plasma," *Proceedings of SPIE - The International Society for Optical Engineering* 8338, 83381H (2011).
- [9] Angelsky, O. V., Ushenko, Y. A., Dubolazov, A. V., Telenha, O. Yu., "The interconnection between the coordinate distribution of Mueller-matrixes images characteristic values of biological liquid crystals net and the pathological changes of human tissues," *Advances in Optical Technologies*, 130659 (2010).
- [10] Ushenko, A. G., Olar, O., "Differential diagnostics of aseptic and septic loosening of the cup of the endoprosthesis of the artificial hip joint by the methods of polarisation tomography," *Informatyka, automatyka, pomiary w gospodarce i ochronie środowiska* 9(3), 22-25 (2019). <https://doi.org/10.35784/iapgos.237>
- [11] Dubolazov, A. V., Marchuk, V., Olar, O. I., Bachinskiy, V. T., Vanchuliak, O. Ya., Pashkovska, N. V., Andriychuk, D., Kostyuk, S. V., "Multiparameter correlation microscopy of biological fluids polycrystalline networks," *Proceedings of SPIE - The International Society for Optical Engineering* 9066, 90661Y (2013).